IEEE Access
Multidisciplinary | Rapid Review | Open Access Journal

Received January 3, 2019, accepted January 21, 2019, date of publication February 4, 2019, date of current version February 22, 2019.

Digital Object Identifier 10.1109/ACCESS.2019.2897110

Underwater Decode-Interleave-Forward Cooperative Strategy for Underwater Acoustic Communication

ZHIYONG LIU, (Member, IEEE), FAN BAI, AND LIZHONG SONG
School of Information Science and Engineering, Harbin Institute of Technology, Weihai 264209, China

Corresponding author: Zhiyong Liu (lzyhit@hit.edu.cn)

This work was supported in part by the National Natural Science Foundation of China under Grant 61871148 and Grant 61201145, and in part by the Shandong Provincial Natural Science Foundation under Grant ZR2016FM02.

ABSTRACT To overcome the problem caused by the large propagation delays of underwater acoustic channel, an asynchronous underwater decode-interleave-forward (UDIF) cooperative strategy is considered for the underwater acoustic cooperative communication system. The UDIF strategy is designed to realize the cooperative transmission and to decrease the end-to-end delay. Aiming at the strategy, a joint multi-branch combining and turbo equalization detector is proposed. To compensate the channel effects and achieve the diversity gain, the turbo equalization, multiuser detection, and combining technique are jointly realized. In the implementation of the detector, the detector is iteratively adapted by switching soft information according to log-likelihood ratio estimates with the turbo processing stage. Moreover, at each iteration, the combining coefficients for the received signals from the source and relay nodes are updated based on the steady-state mean square error, and thus, the proposed detector can effectively combine the received signals without the assumption that full and perfect channel state information of all the links at the receiver is known. The simulation results validate the feasibility and show the advantages of the proposed detector against existing counterparts.

INDEX TERMS Underwater acoustic cooperative communication, asynchronous underwater decode-interleave-forward (UDIF), multi-branch combining, turbo equalization.

I. INTRODUCTION

Underwater acoustic cooperative communication (UACC) is a promising physical layer solution to improve the reliability of underwater acoustic communication systems [1], [2]. However, communication in underwater environments is characterized by large propagation delay, multipath propagation and limited bandwidths [3], which impose new challenges and render technologies designed for terrestrial radio communication not applicable for underwater acoustic communication.

In the UACC, the message sent by source node arrives at destination node through diverse paths, one directly from source and others through relay nodes. Therefore, to achieve better system performance, cooperative strategy, combining technique and detection technique are needed to jointly consider according to the propagation characteristics of underwater acoustic channel. For the cooperative strategy, synchronous amplify-and-forward (AF) and decode-and-forward (DF) cooperative strategy are first applied in underwater acoustic communication in [4]–[6]. However, considering the variable and large propagation delay of underwater acoustic channel, time synchronization among nodes is quite costly. Besides, the length of each time slot that is required to accommodate the maximum link propagation delay will make channel efficiency quite low. Moreover, the mobility of the water and the variance of the sound speed may cause the propagation delay among nodes to vary with time, which render the length of each time slot for synchronized cooperative transmission difficult to determine. Therefore, synchronous cooperation in underwater acoustic network (UAN) is difficult to implement. Asynchronous underwater AF (UAF) and underwater DF (UDF) are proposed in [7], in UAF and UDF, the relay node simply processes the signals received

The associate editor coordinating the review of this manuscript and approving it for publication was Sanaa Sharafeddine.

from source and retransmits it to the destination immediately, instead of retransmitting in the next time slot as in AF and DF. However, the implementation of UAF and UDF assumes that no interferences exist in the received signals from source and relay nodes at the destination node, including inter data-packet interference and inter symbol interference (ISI). Moreover, in [7], performance evaluation is based on theoretical derivation, and no corresponding detector is proposed. In fact, for high data rate UACC, due to the long delay and multipath delay characteristic of underwater acoustic channel, inter data-packet interference and ISI inevitably exist in the received signals.

The situation is further deteriorated if multiple users are present simultaneously in both time and frequency, multiple access interference (MAI) would also be contained in the received signals. The UDF proposed for single-user situations in [7] is not directly applicable. Due to the large delay spread and limited bandwidth of underwater acoustic channel, interleave-division multiple access (IDMA) can be considered to apply in the underwater acoustic communication. Because the IDMA system employs user specific chip interleavers, and can exploits full band-width expansion for coding, these features facilitate chip-based strategies and maintain good performance with far lower complexity than the CDMA scheme [8]. Therefore, in UACC, to achieve diversity gain, besides the detection and extraction for signals of source and relay nodes from the received signals at destination node should be considered, both intersymbol inteference (ISI) and multiple-access interference (MAI) should also be considered to mitigate. In order to remove MAI and ISI, chip-level adaptive decision feedback equalization based on interleave-division multiple access (DFE-IDMA) and code-division multiple access (DFE-CDMA) have been used for multiuser communication in [9]. An adaptive chip-level DFE receiver for a two-user uplink IDMA system has been studied in [10]. In [9] and [10], the researches aim at the non-cooperative communication system, which means that no relay takes part in the information transmission.

For the combining technique, the combing for multiple received signals from different nodes would partly influence the system performance, most of existing studies in UACC adopt equal gain combining (EGC) [5], [11]–[16] or maximum ratio combining (MRC) [11], [17]–[21]. The MRC approach can achieve better performance. However, the MRC assumes that all the channel state information (CSI) of all the paths is known. For practical underwater acoustic cooperative communication system, these CSIs are difficult to obtain.

In this paper, we firstly propose an asynchronous underwater decode-interleave-forward (UDIF) cooperative strategy for underwater acoustic cooperative communication. Then, for the proposed UDIF strategy, a joint multi-branch combining and turbo equalization detector (JMC-TED) is proposed correspondingly. Both the relay strategy and detector are designed according to the characteristics of the underwater acoustic channel. The main contributions of this paper are as follows.

- We propose an asynchronous UDIF cooperative strategy for underwater acoustic cooperative communication system. Unlike the existing UDF strategy, UDIF is the combination of UDF and interleaving technique, and thus can be applied to multi-user situations. For UDIF, the relay node firstly decodes the received signal from source node, and then use its own interleaving sequence to process the decoded signal, this means that different interleaving sequences are used by source and relay nodes. At the destination node, the received signals from the source and relay nodes can be viewed as coming from different users, therefore, even if there is interferences between the data packets, the signals of source and relay nodes can still be extracted according to the difference of interleaving sequences. Meanwhile, the proposed scheme can also reduce the end-to-end delay. This is because the relay node will immediately retransmits the received signals from source to the destination as in UDF.
- Aiming at the UDIF cooperative strategy, we proposed a JMC-TED. The detector will combine multi-branch combining (MC), turbo equalization and multiuser detection into a single robust receiver. Because different interleaving sequences are used by source and relay nodes, the received signals cannot be directly combined, the combination of signals is implemented after the deinterleaving process. The combining coefficients is obtained based on the output steady-state mean square error (SMSE) of each branch of detector, and updated at each iteration of turbo processing. As a result, the proposed MC can adaptively combine multiple inputs via diverse paths, and doesn't require to know the CSIs of all links. Hence, the proposed detector is more suitable for practical UACC systems.

The rest of this paper is organized as follows. Section II presents the considered system model and UDIF cooperative strategy. Section III describes the proposed joint multi-branch combining and turbo equalization detector in details. The simulation results are given in Section IV. Finally, conclusions are drawn in Section V.

II. SYSTEM MODEL AND UNDERWATER DECODE-INTERLEAVE-FORWARD COOPERATIVE STRATEGY

A. SYSTEM MODEL

Consider a asynchronous underwater acoustic cooperative network, as shown in Fig. 1, consisting of K source node S_k ($k = 1, 2, 3, ..., K$), one UDIF relay node R and one destination node D, where S_1 transmits its information to D with the aid of the UDIF relay R. All the nodes work in the half-duplex mode, each of the nodes is equipped with a single transmit and receive element. We assume that all the received packets of relay and destination nodes are fully synchronized.

The corresponding channel coefficient between node i and j is denoted by h_{ij}, where $i, j \in \{S_k, R, D\}$, the channel impulse response $h_{ij}(t)$ can be obtained by a statistical underwater acoustic channel model [3]. Without loss of

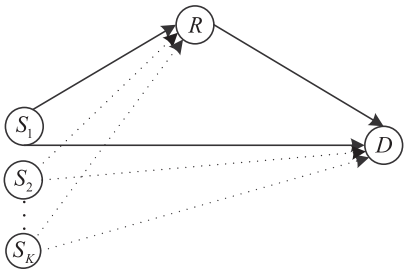

FIGURE 1. Diagram of UACC system.

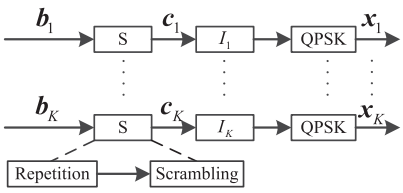

FIGURE 2. Transmitter structure of IDMA.

generality, additive white Gaussian noise (AWGN) is assumed in each link. We assume that all nodes have the same average power constraint. We also assume that IDMA [8] is adopted. The transmitter structure for the source nodes is showed in Fig. 2. Let $b_k = [b_k(1), b_k(2), \cdots, b_k(N_b)]^T \in \{0,1\}_1^{N_b}$ denotes information bits of the kth source node, where $b_k(n) \in \{0,1\}$, N_b is the number of information bits. Firstly, the b_k is encoded by a rate R_c scrambling repetition code, which is utilized to give the system MAI protection, generating a coded sequence

$$c_k = [c_k(1), c_k(2), \cdots, c_k(N)]^T \tag{1}$$

where N is the encoded frame length, $N = N_b F$, F represents the spreading factor. Then, the coded bits are additionally interleaved by user-specific interleaver $I_k[\cdot]$, the interleaving operation disperses the encoded sequence c_k, so that the adjacent chips are approximately uncorrelated. Next, the outputs of interleavers are mapped to quadrature phase-shift keying (QPSK) symbols

$$x_k(t) = A_k \sum_{m=1}^{N_q} d_k(m) g(t - mT) \tag{2}$$

where $d_k(m)$ denotes the mth coded chip bits for the QPSK data streams of the kth user, N_q is the number of chip bits after QPSK modulation, $N_q = N/2$, A_k is the transmitted signal amplitude of the kth user, T is the symbol duration, $g(t)$ denotes the raised cosine pulse, which is a real function, time-limited to the interval $[0, T]$, and normalized, i.e., $\int_0^T g^2(t)dt = 1$. Note that the spreading unit is same for all sources, and it can be equally represented as an ensemble of a bit-repetition operation and a scrambling unit. Distinct interleaver patterns are used to separate different users. These interleavers are generated randomly and independently.

B. UNDERWATER DECODE-INTERLEAVE-FORWARD COOPERATIVE STRATEGY

Due to the long propagation delay characteristic of underwater acoustic channel, we propose a UDIF cooperative strategy for UACC. In the traditional DF, the relay node firstly processes the signals received from source and then retransmits it to the destination in the next time slot, while in UDF, the relay retransmits immediately, instead of retransmitting in the next time slot, as shown in Fig. 3 (a) and (b). In contrast to the UDF, the proposed UDIF strategy doesn't generate more end-to-end delays than UDF. Moreover, the demand for the distances among the nodes is not strict as in UDF, which has corresponding requirements for the distance between nodes to avoid the overlapping of received signals from source and relay nodes. Thus, the less end-to-end delay can be obtained by the proposed UDIF.

In the proposed UDIF cooperative strategy, we assume that the relay node is located between source and destination node. Without loss of generality, we also assume that node S_1 is expected user. d_{S_1R}, d_{RD} and d_{S_1D} denote the distances of $S_1 \to R$, $R \to D$ and $S_1 \to D$, the distances needs to satisfy the conditions of $d_{S_1R} < d_{S_1D}$ and $d_{RD} < d_{S_1D}$. To avoid the problem of error propagation as much as possible, we assume $d_{S_1R} < d_{RD}$ to ensure that the channel of $S_1 \to R$ has high instantaneous signal-to-noise ratio (SNR).

To complete one packet transmission, two stages are required by the UDIF, the process is as follows.

1) Broadcasting Phase

Source node S_1 broadcasts its signal to the relay and D. The transmitted signal of S_1 is generated according to IDMA transmitter procedure, as shown in Fig. 2. The interleaver $\{I_1\}$ should be different from the other nodes. In the proposed UDIF, the received signals at the relay node can be written as

$$r_R(t) = \sum_{k=1}^{K} r_{S_kR}(t - \tau_{S_kR}) + v_R(t) \tag{3}$$

where $r_{S_kR}(t) = \sqrt{P_{S_k}} h_{S_kR}(t) * x_k(t)$, $r_{S_kR}(t)$ denotes the received signal from node S_k, P_{S_k} is transmitted signal power of the kth source node, $h_{S_kR}(t)$ denotes underwater acoustic channel impulse responses from S_k to the relay node, τ_{S_kR} is the asynchronous delay for $S_k - R$, $v_R(t)$ represents samples of the additive white Gaussian noise with zero mean and variance σ_R^2. For the transmitted signal of S_1, the corresponding received signal at the destination node can be expressed as

$$r_{S_1D}(t) = \sqrt{P_{S_1}} h_{S_1D}(t) * x_1(t) \tag{4}$$

where P_{S_1} is transmitted signal power of node S_1, $h_{S_1D}(t)$ denotes underwater acoustic channel impulse responses from S_1 to the destination node.

2) Relaying Phase

After receiving signals from S_1, the relay node first decodes the received signal. Then, it re-processes the information bits with the IDMA transmitter in Fig. 2 to form the transmitting signals of relay, and immediately retransmits the signals

to D. Let $x_R(t)$ expresses the transmitted signal of relay node, the received signal $r_{RD}(t)$ at the destination node can be given by

$$r_{RD}(t) = \sqrt{P_R} h_{RD}(t) * x_R(t) \tag{5}$$

where P_R is transmitted signal power of the relay node, $h_{RD}(t)$ denotes channel impulse responses from node R to D. Thus, the received signal at the destination node can be expressed as

$$r(t) = r_{S_1D}\left(t-\tau_{S_1D}\right) + r_{RD}\left(t-\tau_{RD}\right) + \sum_{k=2}^{K} r_{S_kD}(t-\tau_{S_kD}) + v(t) \tag{6}$$

where $r_{S_kD}(t) = \sqrt{P_{S_k}} h_{S_kD}(t) * x_k(t)$, $h_{S_kD}(t)$ denotes channel impulse responses from node S_k to D, $k \in \{S_2, \cdots, S_K\}$, τ_{iD} is the asynchronous delay for $i - R$, $i \in \{R, S_1, \cdots, S_K\}$, $v(t)$ represents samples of the additive white Gaussian noise with zero mean and variance σ^2.

The key principle of UDIF is that the interleavers of source and relay nodes should be different, this means that the source and relay nodes use different interleaving operation to permute the same encoded sequence. When source and relay nodes broadcast information of source node, in the view of destination node, the received signals from different nodes adopt different interleaver and thus can be viewed as a virtual multiuser IDMA signal, the signal of different nodes can be distinguished and extracted according to the difference of interleaving sequence. Despite the signals sent by source (x_1) and relay nodes (x_R) are different, the transmitted information is the same, to achieve the diversity gain, the combination of signals from source and relay nodes can be implemented after the deinterleaving process, because the only difference between the x_1 and x_R is that the different interleaving sequences are used, more detailed description would be given in the section III.

C. END-TO-END DELAY COMPARISON OF DIFFERENT COOPERATIVE STRATEGIES

In view of the slow speed of sound waves, the decrease of end-to-end delay in underwater acoustic transmission is essential. In tradition synchronous DF strategies, as shown in Fig. 3(a), cooperative transmission is implemented in two time slots. In the time slot 1, the data packet is transmitted by the source node to the relay and destination nodes, respectively. In the time slot 2, the packet received by the relay node is sent to the destination node. Because the length of each time slot is required to accommodate the maximal link propagation delay, thus, the synchronous cooperation is extremely inefficient. The end-to-end delay for cooperative transmission is equal to two times the length of a time slot.

Compared with the synchronous DF strategy, in the asynchronous cooperative strategy (UDF and UDIF), the relay retransmits the signals immediately, instead of retransmitting in the next time slot, thus, the end-to-end delay can be reduced. In the cooperative transmission, there are three links,

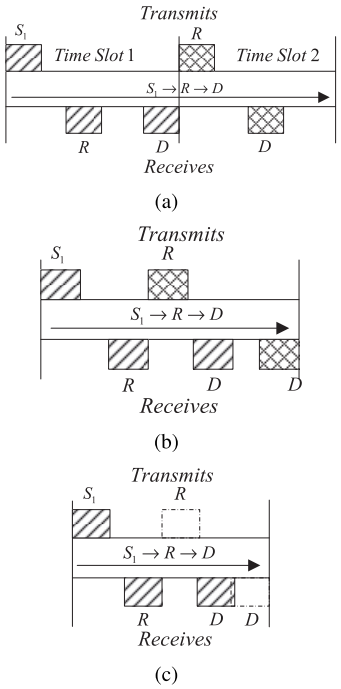

FIGURE 3. Comparison of cooperative transmission strategies: (a) DF; (b) UDF; (c) UDIF.

we use d_{S_1R}, d_{RD} and d_{S_1D} to represent the distances of $S_1 - R$, $R - D$ and $S_1 - D$ link, respectively. The end-to-end delay D_{asyn} required for a data packet transmission can be expressed as $\max\left\{(d_{S_1R} + d_{RD})/c, d_{S_1D}/c\right\}$, where c denotes the sound speed. According to the system model showed in Fig. 1, the distances always meet $d_{S_1R} + d_{RD} \geq d_{S_1D}$. Therefore, D_{asyn} satisfies $D_{asyn} \geq d_{S_1D}/c$. For the limit case, when S_1, R and D are located in a straight line and the relay node R is between S_1 and D, D_{asyn} is equal to d_{S_1D}/c.

For UDF, it is assumed that the ISI, MAI and inter data-packet interference are not existent. Moreover, UDF is proposed for single-user scenarios and is not suitable for multi-user scenarios. In the proposed UDIF, the end-to-end delay can still be decreased as UDF. In addition, because we can use different interleavers to separate the multiple useful copies as well as interferences, the demand for the distances among the S_1, R and D is not strict as in UDF, which has corresponding requirements for the distance between nodes to avoid the overlapping of received signals from source and relay nodes. In our scheme, even if the received signals from source and relay nodes are completely superimposed, the proposed detector can still detect the desired information effectively. Therefore, the end-to-end delay can be further reduced.

III. JOINT MULTI-BRANCH COMBINING AND TURBO EQUALIZATION DETECTOR

Aiming at the proposed UDIF cooperative strategy, the JMC-TED is motivated. The proposed detector structure is depicted in Fig. 4. Note the difference from the

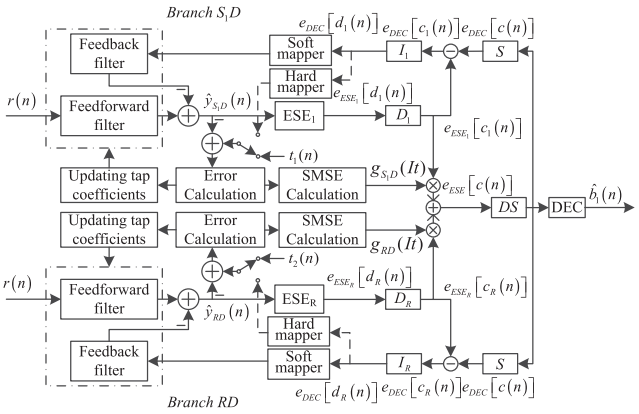

FIGURE 4. The structure of JMC-TED.

conventional detector (single user and single branch) in point-to-point communication, (1) the proposed detector is designed for UACC system with UDIF cooperative strategy, both ISI and MAI are needed to mitigate, (2) the number of branches of detector is greater than 1, to achieve the diversity gain, the output signals from multiple branches should be effectively combined. The proposed detector will combine turbo equalization, multiuser detection (MUD) and combining technique into a single robust receiver. When the number of branch is 1, the JMC-TED becomes a single-branch turbo equalization detector (SB-TED). For relay node, the received signal $r_R(t)$ is firstly processed by the SB-TED, and then immediately retransmits the signals to D after the process of transmitter of relay node. Since the SB-TED is a special case of JMC-TED, in the following content of this section, we will only describe the implementation of JMC-TED in detail. When the branch number is set as 1, the JMC-TED turns into a SB-TED.

In the JMC-TED, the received signal $r(n)$ is firstly processed by the FS-DFE of corresponding branch i as shown in the dotted line box of Fig. 4, $i \in \{S_1D, RD\}$. Then, the output of the FS-DFE is used as the input of elementary signal estimator (ESE) ESE_j, a turbo-type iterative process is applied to process the LLRs generated by the ESE and DEC until a suitably chosen convergence criterion is achieved. The detailed descriptions were given as below.

A. ADAPTIVE FRACTIONALLY SPACED DECISION FEEDBACK EQUALIZATION

The chip-level fractionally spaced decision feedback equalization (FS-DFE) is shown in the dotted line frame of Fig. 4. In the FS-DFE, feedforward filter (FFF) adopts fractionally spaced filter structure, while feedback filter (FBF) uses chip interval. The FS-DFE will directly process the sampled signals after the analog-to-digital converter (A/D), the sampling period is T_s. For $r(t)$, the input signal of detector is $r(n)$, the corresponding branch of detector will process the signal, respectively. In the equalizer, for each branch, the estimation for tap coefficient vector of FFF is given by

$$\hat{w}_i(n) = [\hat{w}_{i,1}(n), \hat{w}_{i,2}(n), \cdots, \hat{w}_{i,L_i}(n)]^H \tag{7}$$

where $i \in \{S_1D, RD\}$, $\hat{w}_i(n)$ is initialized with $\hat{w}_i(0) = [0, 0, \cdots, 0]^H$, L_i is the tap-length of FFF. The tap coefficient vector of FBF can be represented with $\hat{f}_i(n)$, whose dimensions is $M_i \times 1$, $\hat{f}_i(n)$ is also initialized with $\hat{f}_i(0) = [0, 0, \cdots, 0]^H$. The signal vector for FFF of corresponding branch is defined as

$$u_i(n) = [r(n-1), r(n-2), \cdots, r(n-L_i)] \tag{8}$$

where $i \in \{S_1D, RD\}$. $u_{b,i}(n)$ is used to denote the feedback signal vector for FBF, the tap-length is M_i. Thus, the output of the FS-DFE is calculated as

$$\hat{y}_i(n) = u_i(n)\hat{w}_i(n) - u_{b,i}(n)\hat{f}_i(n) \tag{9}$$

In the training mode, the desired signal and the feedback signal are precisely, thus, the corresponding error can be given by

$$e_i(n) = t_i(n) - \hat{y}_i(n) \tag{10}$$

where $i \in \{S_1D, RD\}$, $t_i(n)$ is training sequences, which is different from the other nodes. In order to suppress the ISI, the MMSE criterion for FS-DFE is defined as [9]

$$J_i(n) = \min_{\hat{w}_i(n)} E\left\{|e_i(n)|^2\right\} \tag{11}$$

MSE minimization can be simplified by employing an iterative procedure using a stochastic algorithm. The normalized LMS (NLMS) algorithm is used to resolve the minimization problem.

$$\hat{w}_i(n+1) = \hat{w}_i(n) + \frac{\mu_i}{\delta_i + \|u_i(n)\|^2} e_i(n)u_i(n) \tag{12}$$

$$\hat{f}_i(n+1) = \hat{f}_i(n) + \frac{\mu_{b,i}}{\delta_{b,i} + \left\|u_{b,i}(n)\right\|^2} e_i(n)u_{b,i}(n) \tag{13}$$

where μ_i, $\mu_{b,i}$, δ_i and $\delta_{b,i}$ are positive constant, μ_i and $\mu_{b,i}$ are step-size factor, which are used to respectively control the change in tap coefficients vector of FFF and FBF from one iteration to the next, δ_i is introduced to overcome the problem of numerical calculation difficulty that may arise when $\|u_i(n)\|^2$ is small, $\delta_{b,i}$ is also used to resolve similar problem when $\left\|u_{b,i}(n)\right\|^2$ is small.

After the training stage, the obtained tap coefficient vector is used to process the next received signals, which contain the transmitted data information. It is worth noting that due to the lack of feedback information, in the first iteration, the received signals containing the data information are only processed by the FFF. The obtained tap coefficient vector $\hat{f}_i(n)$ for FBF is set as the initial value of FBF in the following iteration process.

B. JOINT MULTI-BRANCH COMBINING AND TURBO EQUALIZATION DETECTOR

In the following iteration procedure, the detector only processes the received signals containing the data information. The turbo equalization detector (TED) is used to separate the equalized mixed signal $\hat{y}_i(n)$ coming from the FS-DFE of each branch and decode the transmitted data of expected user. During each iteration, the output $\widehat{y}_i(n)$ of FS-DFE is updated according to the feedback information $e_{DEC}\left[d_j(n)\right]$ and the hard mapping of $e_{DEC}\left[d_j(n)\right]$. TED mainly contains two parts, i.e., an elementary signal estimator (ESE) and K single-user a posteriori probability (APP) decoders (DECs). Via the processing of FS-DFE, the ideal equalization performance cannot be obtained, in the soft output $\hat{y}_i(n)$, besides the desired signal, it also contains residual distortion, and thus we may represent the $\hat{y}_i(n)$ as

$$\hat{y}_i(n) = d_j(n) + \zeta_j(n) \tag{14}$$

where i is S_1D as $j = 1$, or i is RD as j is R, $\zeta_i(n)$ is residual distortion, and is composed of residual MAI $\eta_i(n)$ and the noise signal $v_i(n)$. The ESE generates logarithmic likelihood ratio (LLR) which can be obtained according to [8]

$$e_{ESE_j}\left[d_j^I(n)\right] = \frac{2\left\{\hat{y}_i^I(n) - E\left[\zeta_i^I(n)\right]\right\}}{Var\left[\zeta_i^I(n)\right]},\ \forall n \tag{15}$$

where i is S_1D as $j = 1$, or i is RD as j is R, $E[\cdot]$ and $Var[\cdot]$ represent the mean and the variance function, respectively, $d_j^I(n)$, $\hat{y}_i^I(n)$ and $\zeta_i^I(n)$ denote the real part of $d_j(n)$, $\hat{y}_i(n)$ and $\zeta_i(n)$, respectively. The mean and the variance of $\hat{y}_i(n)$ can be obtained by

$$E\left[\hat{y}_i(n)\right] = E\left[d_j(n)\right] + E\left[\eta_i(n)\right], \forall n \tag{16}$$

$$Var\left[\hat{y}_i(n)\right] = Var\left[d_j(n)\right] + \sigma_v^2, \forall n \tag{17}$$

where i is S_1D as $j = 1$, or i is RD as j is R, σ_v^2 is the variance of total noise, the noise $v(n)$ is not available, and thus is replaced with the error signal in (10), the estimation for σ_v^2 can be computed by time averaging the squared error as in [9]

$$\hat{\sigma}_v^2 = \sigma_e^2 = E\left[|e_i(n)|^2\right] \tag{18}$$

Similary, the mean of residual MAI $\eta_i(n)$ is also difficult to obtain, here, we use the mean of error signal of (10) to replace the mean of $\eta_i(n)$, the method of time averaging is similarly adopted to calculate the estimation

$$E\left[\hat{\eta}_i(n)\right] = E\left[e_i(n)\right] \tag{19}$$

In the iterative process, the $E[\zeta_i(n)]$ and $Var[\zeta_i(n)]$ are obtained by

$$E\left[\zeta_i(n)\right] = E\left[y_i(n)\right] - E\left[d_i(n)\right] \tag{20}$$

$$Var\left[\zeta_i(n)\right] = Var\left[y_i(n)\right] - Var\left[d_i(n)\right] \tag{21}$$

The mean and the variance of $d_j(n)$ in (16) and (17) can be calculated by

$$E[d_j^I(n)] = \tanh\{e_{DEC}[d_j^I(n)]/2\}, \forall n \tag{22}$$

$$Var\left[d_j^I(n)\right] = 1 - \left\{E\left[d_j^I(n)\right]\right\}^2, \forall n \tag{23}$$

where $e_{DEC}\left[d_j^I(n)\right]$ is extrinsic logarithmic likelihood ratio (LLR) of $d_j^I(n)$. Initially, we set $E[d_j(n)] = 0$ and $Var[d_j(n)] = 1$ for $\forall j, n$, implying no information from DECs. $e_{DEC}\left[d_j^I(n)\right]$ can be calculated by the difference of $e_{DEC}\left[c^I(n)\right]$ and $e_{ESE_j}\left[c_j^I(n)\right]$, and is followed by the interleaver as

$$e_{DEC}\left[d_j^I(n)\right] = I_j\left\{e_{DEC}\left[c^I(n)\right] - e_{ESE_j}\left[c_j^I(n)\right]\right\} \tag{24}$$

where I_j denotes the user-specific interleaver, $j \in \{1, R\}$, $e_{ESE_j}\left[c_j^I(n)\right]$ represents the deinterleaved output for $e_{ESE_j}\left[d_j^I(n)\right]$, $e_{DEC}\left[c^I(n)\right]$ denotes the output of $e_{ESE}[c(n)]$ after deinterleaving and spreading with the same spreading codeword.

In the detector, $e_{DEC}\left[d_j(n)\right]$ is used as a priori information in ESE for the next iteration. As mentioned above, DEC treats the output of the ESE as its input, and vice versa. During iterative operation, DEC constantly exchanges LLR information with ESE. The estimation $\hat{d}_j(n)$ for $d_j(n)$ can be obtained by hard mapping with the sign function

$$\hat{d}_j(n) = sgn(e_{DEC}[d_j^I(n)]/2) \tag{25}$$

where $sgn(\cdot)$ is the sign function. The QPSK symbols $\hat{d}_j(i)$ can then be despread, deinterleaved and demodulated to recover the information bits $\hat{b}_j(n)$.

It should be noted that the interleavers used by the source and relay nodes is different in the UDIF cooperative strategy. Due to the difference of interleavers (I_1 and I_R), although the same bit information is included in the transmitted signal of source and relay nodes, the different interleaving operations bring different dispersion processing for the same coded sequence c_j. Therefore, the outputs ($\hat{y}_{S_1D}(n)$ and $\hat{y}_{RD}(n)$) of chip-level FS-DFE cannot be directly combined. But the signals of two branches can be combined after the deinterleaving process. This is because the same spreading sequence is adopted in the UACC, the output signals of deinterleaving process for the two branches represent the same transmitted information. For $e_{ESE_j}\left[d_j(n)\right]$, after the deinterleaving, the $e_{ESE_j}\left[c_j(n)\right]$ can be obtained, $j \in \{1, R\}$, and thus the combined signal can be represented as

$$e_{ESE}[c(n)] = g_{S_1D}(It)e_{ESE_1}[c_1(n)] + g_{RD}(It)e_{ESE_R}[c_R(n)] \tag{26}$$

where It denotes the iterative number, $g_{S_1D}(i)$ and $g_{RD}(i)$ represent combining coefficients of the ith iteration for branch S_1D and RD, respectively. The computation of combining coefficients is given in Section C.

For the JMC-TED, the iterative processing effectively exploit the priori information of coded symbols to repeat the equalization and the combination, and improve the performance of detector. In the training mode, the feedback signal in $u_{b,i}(n)$ of (9) are composed with training sequances, thus, the tap coefficient vector $\hat{w}_i(n)$ and $\hat{f}_i(n)$ are adaptively adjusted according to the correct decisions. Nevertheless, in the decision-directed mode, there are no feedback of $e_{DEC}\left[d_j(n)\right]$ ($j \in \{1, R\}$) from the DEC at the first iteration, as a result, the input of FBF is not available. Therefore, at the first iteration ($It = 1$), for the received signal containing the bit informations, only the FFF is used to handle the received signal. Then, the soft output of FFF is given to the ESE_j. The extrinsic information of ESE_j is processed by the deinterleavers, combination and despreader module. The DEC generates the bit-level extrinsic LLRs, which are also processed by the spreader and interleaver. After the process, the $e_{DEC}\left[d_j(n)\right]$ is obtained. Then, the obtained extrinsic information is softly mapped to form new decision symbols $\bar{d}_j(n)$, which are fed back to the FBF. For the soft mapper, the soft chip decisions is defined as

$$\overline{d}_j(n) = \tanh\left\{e^I_{DEC}\left[d_j(n)\right]/2\right\} + j\tanh\left\{e^Q_{DEC}\left[d_j(n)\right]/2\right\} \tag{27}$$

where $e^I_{DEC}\left[d_j(n)\right]/2$ denotes the real part of $e_{DEC}[d_j(n)]$, $e^Q_{DEC}\left[d_j(n)\right]/2$ represents the imaginary part of $e_{DEC}[d_j(n)]$.

When iterative number (It) is greater than 1, the detector works in decision-directed mode, both $\hat{w}_i(n)$ and $\hat{f}_i(n)$ are adjusted using the error signal $e_i(n)$

$$e_i(n) = \tilde{d}_j(n) - \hat{y}_i(n) \tag{28}$$

where $\tilde{d}_j(n)$ is the hard mapping of $e_{DEC}\left[d_j(n)\right]$. For the hard mapper, the sign function (sgn) is used as the mapping function

$$\tilde{d}_j(n) = sgn\left\{e^I_{DEC}\left[d_j(n)\right]/2\right\} + jsgn\left\{e^Q_{DEC}\left[d_j(n)\right]/2\right\} \tag{29}$$

In each iteration, the new priori information is given to the FS-DFE and the TED, the effect of ISI and MAI cancellation can be improved.

C. ACQUISITION OF COMBINING COEFFICIENTS

The steady-state MSE (SMSE) is an important parameter on detection performance. The smaller the value is, the better performance the detector can achieve. In contrast, larger value of SMSE may induce worse performance. Therefore, the combining coefficients can be obtained according to the SMSE, as follows

$$g_i(It) = \frac{e^{-G_i}}{e^{-G_{S_1D}} + e^{-G_{RD}}} \tag{30}$$

where i denotes ith branch, G_i represents the SMSE of ith branch, $i \in \{S_1D, RD\}$. When the iterative number is 1, the estimation for G_i can be calculated by time averaging the squared error in (10)

$$\hat{G}_i = E\left[\left|t_i(n) - \hat{y}_i(n)\right|^2\right] \tag{31}$$

When the iterative number is greater than 1, the estimation for G_i can be obtained by the time averaging the squared error in (28)

$$\hat{G}_i = E\left[\left|\tilde{d}_j(n) - \hat{y}_i(n)\right|^2\right] \tag{32}$$

From (30), it is obvious that the smaller the steady-state MSE is, the larger the combing coefficient g_i can be obtained. In addition, it is noted that the combining coefficients are obtained based on the SMSE, the proposed approach does not need to know the CSIs of all links. Thus, it is more suitable for practical underwater acoustic cooperative systems.

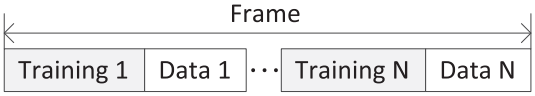

FIGURE 5. Frame structure.

IV. SIMULATION RESULTS

In the simulations, we consider an underwater acoustic cooperative network with K source nodes, one relay and one destination node. We assume that the transmitter and relay have the same powers. The repetition code adopts the same spreading sequence $\{+1, -1, +1, -1, +1, -1, +1, -1\}$ for all users as in [9], the repetition code rate R_c is $1/8$. The size of interleaver is set as 1024. The transmitter uses the QPSK modulation. In order to distinguish different users, random interleavers [8] are adopted. The iteration number of detector is set as 5. For A/D, the sampling frequency f_s is set as 32 kHz. The tap-length L_i of FFF is set to 80 (fractionally spaced sampling), and the tap-length M_i of FBF is set as 10. The frame structure is shown in Fig. 5, a frame consists of N sets of the training symbols and the data symbols, the symbol duration is 1 ms, the length of both training period and data period is set as 128 symbol duration, thus, the date rate is 500 b/s. As seen from Fig. 5, data packets are transmitted continuously, thus, we assume that the received signals from different nodes at the destination node are completely superimposed except for Section IV. E. Due to the operation of spreading, the chip number is 128×8, then via the process of QPSK modulation, the chip number after QPSK changes to 512. For FS-DFE, the μ_i and $\mu_{b,i}$ are set as 0.5 and 0.1, respectively, both δ_i and $\delta_{b,i}$ are set to 0.5.

A. UNDERWATER ACOUSTIC CHANNEL IMPULSE RESPONSE

The underwater acoustic channel is generated with statistical underwater acoustic channel model [3]. In the model, the carrier frequency is set as 12 kHz and the band is limited to 4 kHZ; the depth is set as 30 m, the sources, relay and destination node are positioned at 15 m, 10 m and 5 m

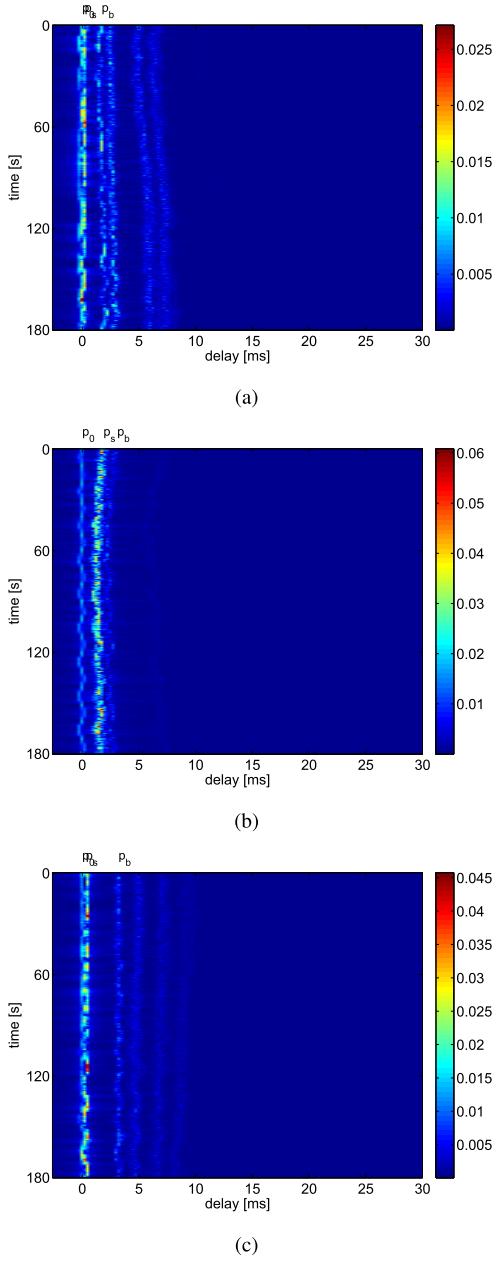

FIGURE 6. Magnitude of channel impulse responses over time-delay domain for different distance: (a) 300 m, the channel of $S_1 - D$; (b) 120 m, the channel of $S_1 - R$; (c) 200 m, the channel of $R - D$.

from the sea surface, respectively; the distances of $S_1 - D$, $S_1 - R$ and $R - D$ are set as 300 m, 120 m and 200m, respectively.

In the Fig. 6, underwater acoustic channel impulse responses of three different distances are shown. It is seen that maximum delay-spread times are about 7, 3 and 8 ms for distance of 300, 120 and 200 m, respectively. In the simulation, the channels are normalized, and we assume that the underwater acoustic channel is quasi-static, which means that in the transmission process of a data packet, the channel is invariant, but for the transmission of next data packet, the channel will change accordingly.

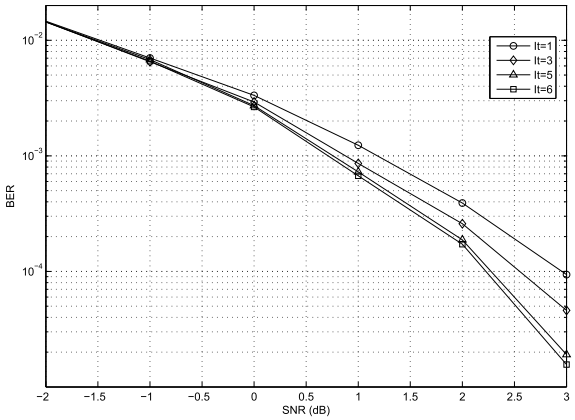

FIGURE 7. The BER performance of SB-TED with different iterative number, K=1.

B. THE EFFECT OF ITERATIVE NUMBER ON BER PERFORMANCE

In this section, the effect of iterative number on BER performance is evaluated. In the simulation, the point-to-point communication between S_1 and D is considered, the receiver adopts the SB-TED. A Monte-Carlo simulation is set up based on the channel in Fig. 6(a). For 500 channel realizations, 500 sets of training sequence and data packet are transmitted. The bit error rate (BER) is obtained by averaging the BER curve on 500 channel realizations.

Fig. 7 shows the effects of iterative number on BER. As seen from the Fig. 7, the iterative number is an important factor on detection performance for the SB-TED. The BER performance of detector is improved evidently with the increasement of iterative number, but most of the iterative gains are obtained in the foremost five iterations. This is because the iterative operation can improve the reliability of feedback information, which in turn decreases the error propagation in the FS-DFE. According to the results in Fig. 7, in the following simulations, five iterations are adopted by the turbo equalization detector.

C. EFFECTIVENESS VALIDATION OF MULTI-BRANCH COMBINING

In the simulation, we assume the SNR (dB) of $r_{S_1D}(n)$ is SNR_{S_1D}, for $r_{S_1R}(n)$, $SNR_{S_1R} = SNR_{S_1D} + 3\ dB$. The point on the BER performance is obtained by averaging the BER curve on 500 data packets, for each data packet, one group channels including h_{S_1D}, h_{S_1R} and h_{RD} is used for simulation, h_{S_1D}, h_{S_1R} and h_{RD} can be obtained from the channels of Fig. 6(a)-(c), respectively. For practical underwater acoustic cooperative communication system, it is difficult to obtain the channel state information (CSI) of all the links, moreover, due to channel variations, the obtained estimation for channels among the nodes maybe have outdated when the CSIs are used to compute the combining coefficients. Therefore, in this paper, we only consider the combining approaches without the assumption that the CSIs should be known beforehand.

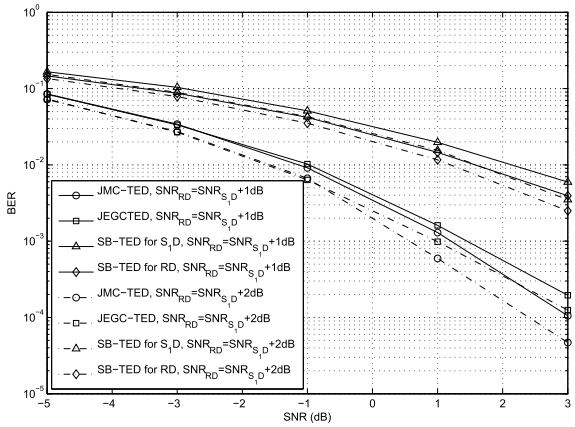

FIGURE 8. Comparison of combination approaches, It=5 and K=1.

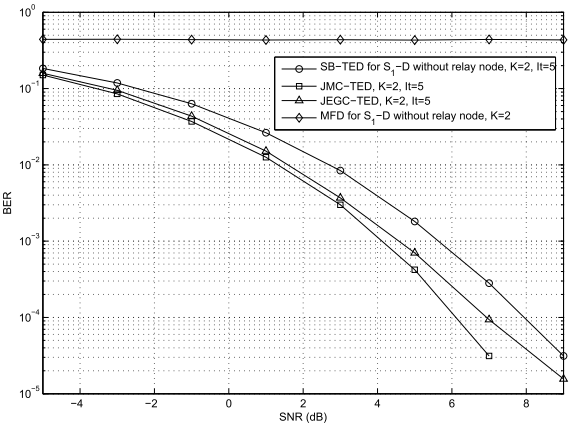

FIGURE 9. BER performance comparison of the proposed detector and existing approaches.

In this section, the performances of two joint combination and turbo equalization detector are compared, one is joint EGC and turbo equalization detector (JEGC-TED), the combining coefficients are set as $g_{S_1D} = g_{RD} = 0.5$, and the other is JMC-TED, the combining coefficients can be obtained by (30).

In Fig. 8, we check the BER performance of two combination schemes, the horizontal axis denotes SNR SNR_{S_1D}. The simulation results of two different SNR SNR_{RD} are given, one is $SNR_{RD} = SNR_{S_1D} + 1\ dB$, the other is $SNR_{RD} = SNR_{S_1D} + 2\ dB$. It is observed that the JMC-TED achieves better BER performance than JEGC-TED. This is because combining coefficients are important factor on BER performance, the JMC-TED uses better combining coefficients than JEGC-TED. It is also seen that the JMC-TED and JEGC-TED achieve much better BER performance than SB-TED, which is used to detect the bit information transmitted by source or relay node from the received signal (the interleaver adopted by source and relay nodes is different). This is because that the JMC-TED and JEGC-TED can obtain the diversity gain by combing the recieved signal from source and relay nodes.

D. COMPARISON OF BER PERFORMANCE OF DIFFERENT METHODS

In the section, we will compare the BER performance of the proposed detector and existing approaches. The BER curve are obtained by averaging the BER curve on each channel realization. In the simulation, K is set as 2, this means that there is a interfere user in the UACC. The channel h_{S_2j} is also generated by the statistical underwater acoustic channel model, and likewise normalized, $j \in \{R, D\}$. We assume that the SNR_{S_1R} satisfies $SNR_{S_1R} = SNR_{S_1D} + 3\ dB$, and the SNR_{RD} satisfies $SNR_{RD} = SNR_{S_1D} + p(j)$, where $p(j)$ is modeled as discrete uniform distribution random variable, $1 \leq p(j) \leq 2$.

Fig.9 shows the BER performance of different approaches. In the UDF [7], no interferences are assumed to be existent, including ISI and MAI, while in the simulation of this section, both the two kinds of interference are existent. For comparison, the matched filter detector (MFD) is also simulated, in which neither ISI nor MAI is considered to mitigate. In the MFD, the received signal firstly be processed by a matched filter, the template signal is obtained by $g(n) * h_{S_1D}(n)$, whose length is also truncated to 80 (the same length as tap-length of FFF); then, the chip-level output of matched filter is processed by demodulation, deinterleaver, despreader and decision blocks, and the bit information sent by the transmitter is eventually recovered. It is observed that the SB-TED achieves significant amount of gains over the MFD. This is because the ISI and MAI cannot be effectively mitigated by MFD. In addition, it is seen that the JMC-TED and JEGC-TED achieves better BER performance than SB-TED. This is because the diversity gain can be obtained by the JMC-TED and JEGC-TED under the cooperation of relay node.

E. BER AND CONVERGENCE PERFORMANCE COMPARISON UNDER DIFFERENT END-TO-END DELAYS

In this section, the effect of end-to-end delay on BER and convergence performance is evaluated. Two limit cases are considered here. One is that the received signals from source and relay nodes are completely superimposed, which means that all the three nodes are located in a straight line and the relay node is between source and relay node. The other is that the received signals from source and relay node are completely separated and the overlapping between them is not existent.

In Fig. 10, we check the BER performance under different end-to-end delays. In the simulation, the SNR_{RD} satisfies $SNR_{RD} = SNR_{S_1D} + 2dB$. It can be observed from Fig. 10 that the BER performance in the case of complete separation is better than that in the case of complete superposition. This is because that the interference between source and relay nodes is caused by the complete superposition of signals. It is also seen that JMC-TED can achieves better performance than MFD-TED. This is because that JMC-TED can effectively

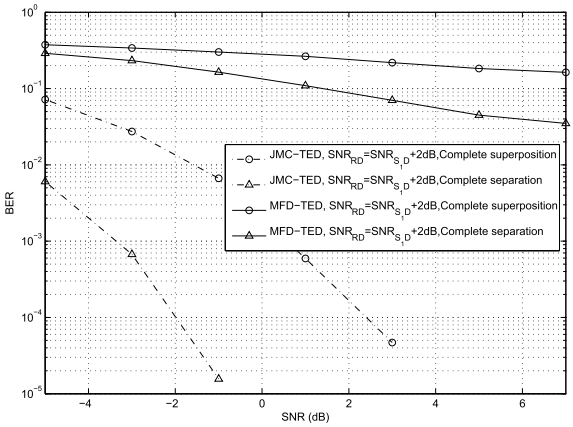

FIGURE 10. BER Performance Comparison under Different end-to-end Delays, It=5 and K=1.

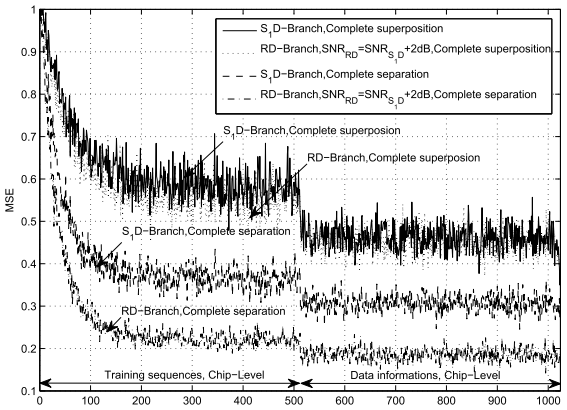

FIGURE 11. Convergence Performance Comparison under Different end-to-end Delays at $SNR_{S_1D} = 3dB$, It=5 and K=1.

mitigate the ISI and MAI. As a result, compared with the MFD-TED, the JMC-TED can still achieve acceptable BER performance under the case of complete superposition, which makes the demand for relay location is not strict as in UDF, the end-to-end delay can be further reduced. Fig. 11 shows the convergence of JMC-TED under two cases. It is seen that compared with complete superposition case, lower MSE performance can be achieved under complete separation case. This is because that complete superposition can cause severe MAI. It is also seen that the achieved steady-state mean square error in the turbo equalization stage is better than that in the training stage. This is because in the turbo equalization stage, with the iteration number increasing, the feedback information becomes more and more accurate, via repeated iterations, the mean square error is further reduced.

F. BER PERFORMANCE COMPARISON UNDER DIFFERENT USER NUMBER

In this section, we will illustrate the effect of user number on the performance of JMC-TED. The channel $h_{S_{ij}}$ is obtained with the statistical underwater acoustic channel model and then normalized, $i \in \{2, 3, ..., K\}$, $j \in \{R, D\}$. The assumption for SNR_{S_1R} and SNR_{RD} is the same as in Fig. 9.

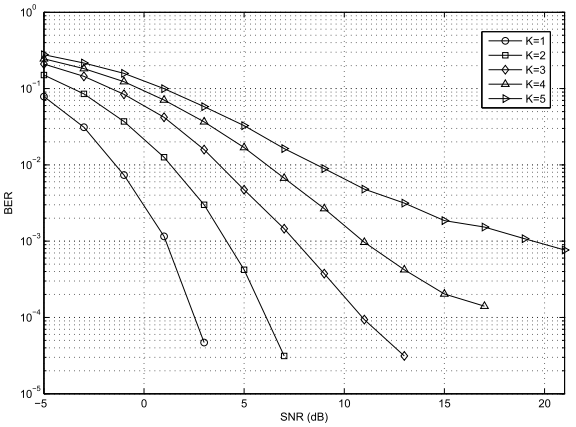

FIGURE 12. BER Performance Comparison under Different User Number.

Fig. 12 shows the BER performance under different number of users. It is observed that the BER performance is gradually degraded as the number of user increases. This is because that MAI will become more and more severe with the increase of number of interfere users.

V. CONCLUSION

We develop a new cooperative strategy (UDIF) for underwater acoustic cooperative communication by considering the large propagation delays of underwater acoustic channel. The main advantage of the proposed strategy is the saving of end-to-end delay and can be applied to multiuser systems. Aiming at the proposed strategy, a JMC-TED, which can jointly implement combining technique, turbo equalization and multiuser detection, has been proposed. Simulation results validate the ability of TED and the feasibility of adaptive multi-branch combing. Simulation results also demonstrate that the proposed detector can achieve better performance than existing counterparts.

ACKNOWLEDGMENT

The authors would like to thank the anonymous referees for their helpful suggestions.

REFERENCES

[1] S. Al-Dharrab, M. Uysal, and T. M. Duman, "Cooperative underwater acoustic communications," *IEEE Commun. Mag.*, vol. 51, no. 7, pp. 146–153, Jul. 2013.
[2] Y. Zhang, Y. Chen, S. Zhou, X. Xu, X. Shen, and H. Wang, "Dynamic node cooperation in an underwater data collection network," *IEEE Sensors J.*, vol. 16, no. 11, pp. 4127–4136, Jun. 2016.
[3] P. Qarabaqi and M. Stojanovic, "Statistical characterization and computationally efficient modeling of a class of underwater acoustic communication channels," *IEEE J. Ocean. Eng.*, vol. 38, no. 4, pp. 701–717, Oct. 2013.
[4] C. Carbonelli and U. Mitra, "Cooperative multihop communication for underwater acoustic networks," in *Proc. 1st ACM Int. Workshop Underwater Netw.*, 2007, pp. 97–100.
[5] M. Vajapeyam, U. Mitra, J. Preisig, and M. Stojanovic, "Distributed space-time cooperative schemes for underwater acoustic communications," in *Proc. OCEANS-Asia Pacific*, May 2007, pp. 1–8.
[6] J.-W. Han, H.-J. Ju, K.-M. Kim, S.-Y. Chun, and K.-C. Dho, "A study on the cooperative diversity technique with amplify and forward for underwater wireless communication," in *Proc. OCEANS-MTS/IEEE Kobe Techno-Ocean*, Apr. 2008, pp. 1–3.

[7] P. Wang, L. Zhang, and V. O. K. Li, "Asynchronous cooperative transmission for three-dimensional underwater acoustic networks," *IET Commun.*, vol. 7, no. 4, pp. 286–294, Mar. 2013.
[8] L. Ping, L. Liu, K. Wu, and W. K. Leung, "Interleave division multiple-access," *IEEE Trans. Wireless Commun.*, vol. 5, no. 4, pp. 938–947, Apr. 2006.
[9] S. A. Aliesawi, C. C. Tsimenidis, B. S. Sharif, and M. Johnston, "Iterative multiuser detection for underwater acoustic channels," *IEEE J. Ocean. Eng.*, vol. 36, no. 4, pp. 728–744, Oct. 2011.
[10] S. N. Qader, C. C. Tsimenidis, B. S. Sharif, and M. Johnston, "Adaptive detection for asynchronous uplink IDMA shallow-water acoustic channels," in *Proc. Sensor Signal Processing for Defence (SSPD)*, Sep. 2012, pp. 1–5.
[11] A. Saif, M. Ismail, R. Nordin, and M. Fadhil, "Performance analysis of relay and combining methods in wireless networks," *J. Theor. Appl. Inf. Technol.*, vol. 75, no. 1, pp. 67–80, May 2015.
[12] Y. Chen, Z. Wang, L. Wan, H. Zhou, S. Zhou, and X. Xu, "OFDM-modulated dynamic coded cooperation in underwater acoustic channels," *IEEE J. Ocean. Eng.*, vol. 40, no. 1, pp. 159–168, Jan. 2015.
[13] B. Karakaya, M. O. Hasna, T. M. Duman, M. Uysal, and A. Ghrayeb, "Multi-resampling Doppler compensation in cooperative underwater OFDM systems," in *Proc. 2013 MTS/IEEE OCEANS-Bergen*, Jun. 2013, pp. 1–8.
[14] S. Yerramalli and U. Mitra, "Optimal power allocation and doppler compensation in cooperative underwater networks using OFDM," in *Proc. OCEANS*, Oct. 2009, pp. 1–6.
[15] S. Al-Dharrab and M. Uysal, "Outage capacity regions of multicarrier DF relaying in underwater acoustic channels," in *Proc. 26th Biennial Symp. Commun. (QBSC)*, May 2012, pp. 30–33.
[16] R. Cao, F. Qu, and L. Yang, "Asynchronous amplify-and-forward relay communications for underwater acoustic networks," *IET Commun.*, vol. 10, no. 6, pp. 677–684, Apr. 2016.
[17] Q. Song and M. Garcia, "Cooperative OFDM underwater acoustic communications with limited feedback," *Int. J. Comput. Appl.*, vol. 54, no. 16, pp. 42–46, Sep. 2012.
[18] A. V. Babu and S. Joshy, "Maximizing the data transmission rate of a cooperative relay system in an underwater acoustic channel," *Int. J. Commun. Syst.*, vol. 25, no. 2, pp. 231–253, Feb. 2012.
[19] X. Cheng, R. Cao, F. Qu, and L. Yang, "Relay-aided cooperative underwater acoustic communications: Selective relaying," in *Proc. Oceans-Yeosu*, May 2012, pp. 1–7.
[20] D. D. Tan, T. T. Le, and D.-S. Kim, "Distributed cooperative transmission for underwater acoustic sensor networks," in *Proc. IEEE Wireless Commun. Netw. Conf. Workshops (WCNCW)*, Apr. 2013, pp. 205–210.
[21] C. Carbonelli, S.-H. Chen, and U. Mitra, "Error propagation analysis for underwater cooperative multi-hop communications," *Ad Hoc Netw.*, vol. 7, no. 4, pp. 759–769, Jun. 2009.
[22] C. Berrou and A. Glavieux, "Near optimum error correcting coding and decoding: Turbo-codes," *IEEE Trans. Commun.*, vol. 44, no. 10, pp. 1261–1271, Oct. 1996.

ZHIYONG LIU was born in Henan, China, in 1979. He received the Ph.D. degree in information and communication engineering from the Harbin Institute of Technology Shenzhen Graduate School, Shenzhen, China, in 2010. From 2010 to 2016, he was a Lecturer with the School of Information Science and Engineering, Harbin Institute of Technology, Weihai, where he is currently an Associate Professor. His research interests include signal processing for wireless communications, cooperative communication, and underwater acoustic communication.

FAN BAI received the B.E. degree in information and communication engineering from Hebei University, Baoding, China, in 2017. She is currently pursuing the M.E. degree with the School of Information and Electrical Engineering, Harbin Institute of Technology, Weihai. Her research interests include cooperative communication, underwater acoustic communication, and multiuser detection.

LIZHONG SONG received the Ph.D. degree in information and communication engineering from the Harbin Institute of Technology, Harbin, China, in 2005. From 2001 to 2012, he was a Lecturer and an Associate Professor with the Harbin Institute of Technology, Weihai, China, where he is currently a Professor. His research interests include wireless communication and networks, antenna design, wireless electromagnetic wave propagation, microwave technology, and radar signal processing.